MODELING AND MEASURING LIMB FINE-MOTOR UNSTEADINESS*

Raymond E. Magdaleno, Henry R. Jex, and R. Wade Allen
Systems Technology, Inc., Hawthorne, California

ABSTRACT

Threading a needle, pointing a flashlight, wielding a soldering iron, taking sextant readings, or aiming a handgun — all are tasks in which limb unsteadiness limits our finesse of visual-motor control. In this paper we examine such "fine-motor unsteadiness" — its properties, conceptual and analytical models, and experimental measurements.

Fine-motor unsteadiness (fluctuations of limb movement about a desired limb position) can have several oscillatory modes, which results in a multi-peaked spectrum and requires a fairly complex model. Based on a data review, the tentative model derived here includes: neuromuscular system (primarily muscles, spindles, tendons, and bones), grip interface, and control system dynamic elements. The properties of this model change with muscle tension and match a wide group of extant data. Particularly interesting is a tendon-compliance mode which seems dominant in the frequently observed "tremor mode" at 10-12 Hz and whose amplitude peak increases with force on the limb.

A simple experiment was performed to investigate the amplitude/force relationships of the "tremor mode." As the finger-pull force increased from 5 to 20 newtons, the tremor mode frequency for a given individual stayed within roughly ±1 Hz over a range from 9-12 Hz, while the average magnitude of the rms tremor acceleration increased tenfold.

A standardized test for making such measurements is given and applications in the fields of psychophysiological stress and strain measurements are mentioned.

INTRODUCTION

Threading a needle, pointing a flashlight, wielding a soldering iron, taking a sextant reading, or aiming a handgun — all are examples of fine-motor tasks in which hand unsteadiness limits our finesse of visual-motor control. To quote Marsden in Ref. 1:

> "Our ability to perform tasks involving manual dexterity is limited by fluctuations in the force of muscle contraction and variations in the position of the hand and fingers which we term physiological tremor. If these fluctuations were totally asynchronous, delicate operations involving the use of both hands would be even more frustrated than if tremor of the two hands were synchronized. By holding a pencil in each hand and trying to keep the points in light contact, it is apparent that the involuntary movements of the two hands are not perfectly synchronous."

Such drift and fluctuations about a desired limb position are defined herein as fine-motor unsteadiness. Generally, these motions can have several oscillatory "modes," depending on the nature of the task. Before meaningful measurements can be made, it is important to understand these modes and their possible interactions. Putting the cart before the horse for tutorial clarity, we will first present our neuromuscular model for fine-motor tasks and then review the data on which it is based. This will lead to a set of simple measurements which can yield the salient characteristics of fine-motor unsteadiness. A brief experiment was made to optimize the proposed measures and procedures and to provide samples of typical data.

NATURE OF UNSTEADINESS

Conceptual and Analytical Models

Figure 1 shows a block diagram of a human operator performing a fine-motor task in which he attempts to minimize a perceived error by manipulating the controlled element in the correct direction.

The major internal functional elements in a human controller are: central sensing and equalization (Y_{CNS}), the muscle/manipulator dynamics (G_m), and the resulting proprioceptive feedback (G_p). Generally, the operator adopts equalization (anticipation lead or something lag) so that the forward loop describing function for the combination of man and controlled element behaves like an integrator in the unity-gain crossover frequency region (i.e., from 0.1 to 1 Hz, Refs. 2 and 3). The man/machine system then has a dominant "visual-motor" closed-loop mode (denoted by subscript CL) just above these frequencies, i.e., f_{CL} = 1-2 Hz. At higher frequencies, other dynamic modes, due to internal neuromuscular system feedbacks, will also be present. These can often be

*This work was sponsored by Lockheed Space and Missle Systems Co., as part of the NASA Manned Spacecraft Center's "Integrated Medical Biological Laboratory Measurement System," under Consulting Subcontract LCS7Z7920K.

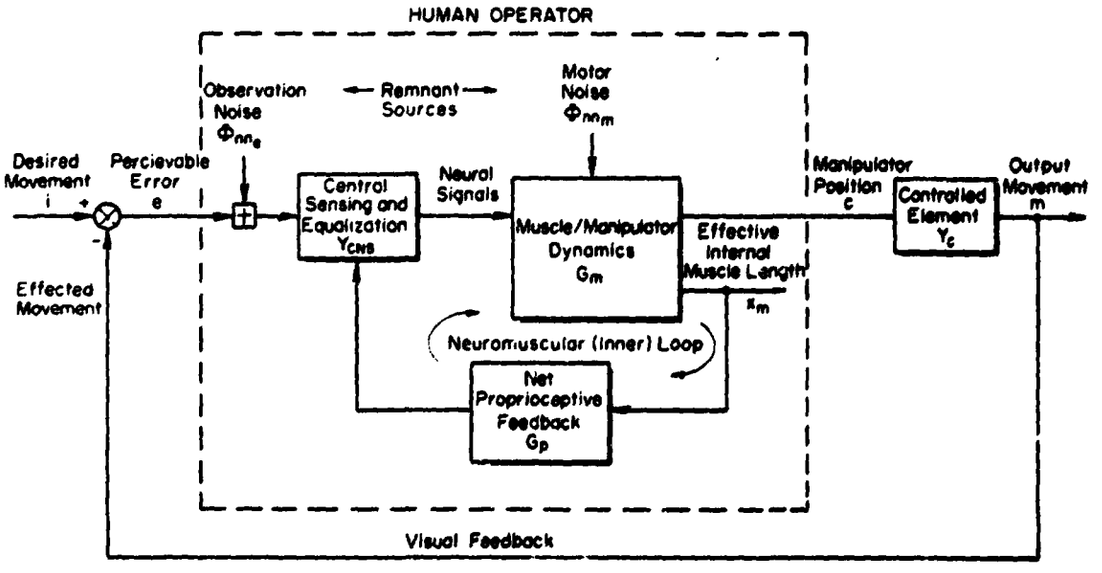

Figure 1. Block Diagram of Human Operator/Controlled Element During Fine-Motor Tasks

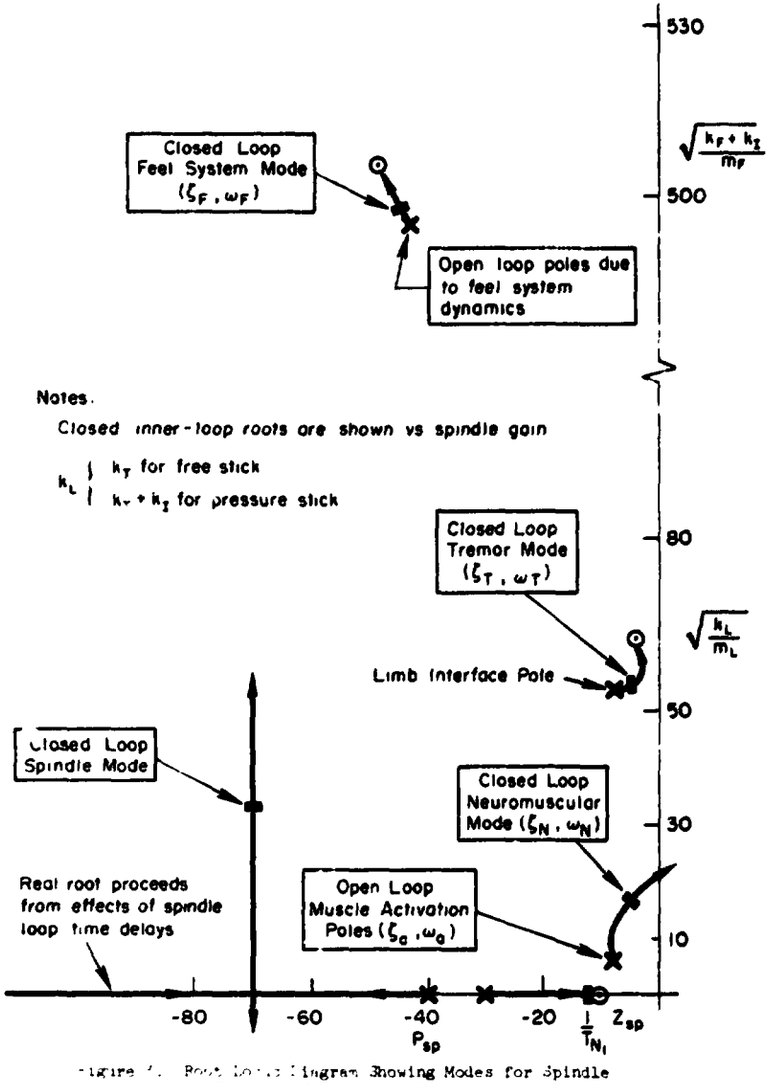

Figure 7. Root Locus Diagram Showing Modes for Spindle Closure of Neuromuscular Loop

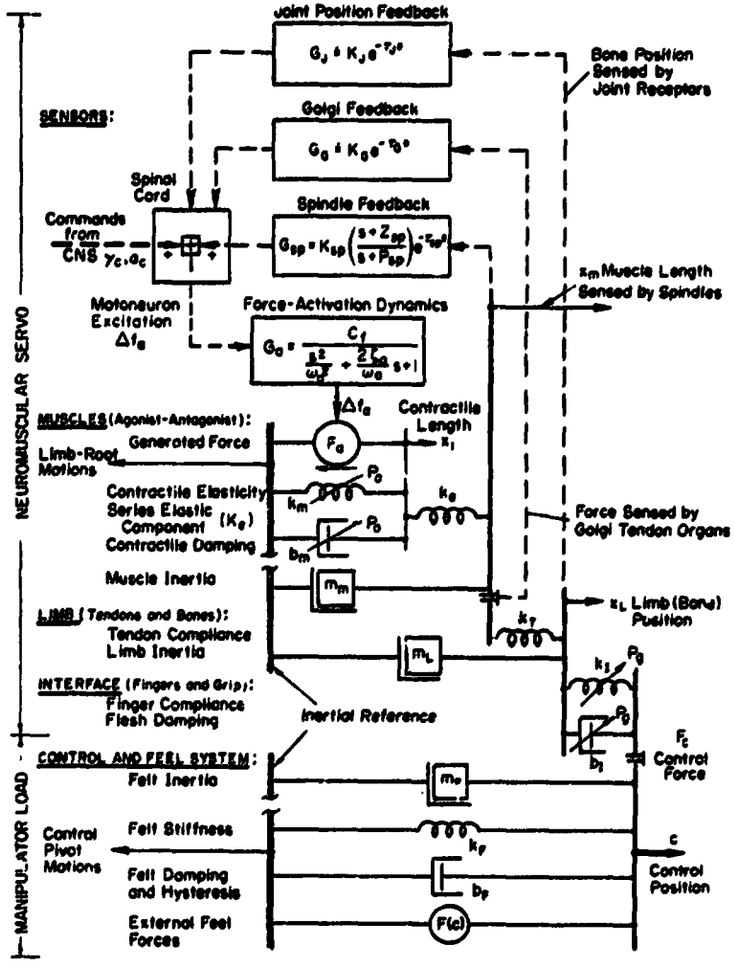

Figure 8. Network Diagram for Combined Neuromuscular Servo and Manipulator System (Shows Elements Required to Represent Neuromuscular and Tremor Modes)

ignored in modeling the manual control of vehicles, but become important during fine-motor tasks.

Proprioceptive information is shown feeding back an internal muscle length change rather than the manipulator position directly (Ref. 2); this has important effects as will be seen shortly. Muscle spindles are the dominant elements in the net proprioceptive feedback. These feed back a dynamically varying internal muscle length due to their location within the active muscle. Golgi tendon organs (force sensors) are also present; their dynamics are quite similar to those for spindles (Ref. 4). Joint angle sensors are present, too, but appear to play only a minor role in fine-motor tasks.

Also shown in Fig. 1 are two sources of remnant (noise) excitation: "observation and processing" noise, Φ_{nn_e}, (Refs. 5 and 6) and "motor remnant," Φ_{nn_m} (Refs. 3 and 5). The latter arises from muscle nonlinearities and irregularities in motor neuron firing rate.

The general form for the power spectral density of the manipulator position is given by:

$$\Phi_{cc} = |G_1|^2 \Phi_{nn_e} + |G_2|^2 \Phi_{nn_m} + |G_{1c}|^2 \Phi_{ii}$$

i.e., each remnant excites some closed-loop transfer function. Note that a peak in Φ_{cc} could be due to either a lightly damped mode in the transfer functions or to a narrowband excitation process in the remnants, or both effects together. Because of the intrinsic nonlinearities in the muscle springiness, damping and neural firing rates, which vary with tension, the dominant modes may be different when tracking (with both agonist and antagonist muscles tensed) than when holding a steady force (with one or the other muscle slack).

To provide an appropriate conceptual and dynamical framework to interpret data, a lumped parameter model has been derived which fits the essential neuromuscular phenomena observed in fine-motor unsteadiness. This model, shown in Fig. 2, reflects a re-interpretation of the data and refinement of the model of Ref. 7, with more detail in representing the limb and muscle inertias, tendon compliance and grip interface compliance and damping. In addition,

we have added the "Activation Dynamics" which reflect the lag and attenuation in converting motorneuron firing rate into generated muscle force. This is the simplest model that can handle limiting cases such as isometric (fixed) and isotonic (free) controls, held objects (like flashlights, soldering irons, etc.), while reflecting the separate "neuromuscular" and higher frequency "tremor" and "manipulator" modes observed in the literature (see the following subsection, "Data on Unsteadiness Power Spectral Density"). Detailed numerical analysis has not yet been carried out for this model, but a brief series of "system surveys" using the systems analysis techniques of Ref. 3 has been made which shows that it yields modes and dynamic parameter trends which fit the large array of extant unsteadiness and tremor spectra.

Typical neuromuscular system modes for the neuromuscular "inner" loop of Fig. 1 are shown in the example root locus diagram of Fig. 3. The muscle spindle and force activation elements dominate the net proprioceptive feedback path. The "Closed-Loop Neuromuscular" mode near 20 rad/sec (3.3 Hz) has been shown (Ref. 7) to arise from the open-loop muscle force activation characteristics measured in experiments. The closed-loop "Tremor" and "Feel" System modes arise from the internal muscle-limb feedbacks and elastic elements, coupled with the control stick and grip compliance properties. It can be shown (e.g., Refs. 2 and 8) that the pole-zero dipoles arise from the spindles feeding back an internal muscle length rather than the manipulator position. This results in two sets of quadratic zeros near the imaginary axis which attract closed-loop roots. The closed-loop Tremor Mode arises from the Limb Interface dipole, which reflects the limb inertial interacting with the Interface, Tendon, and Contractile elements of Fig. 2. The closed-loop Feel System mode arises from the feel system inertia, spring rate, and damping interacting with the interface compliance.

The key feature of the dynamic situation depicted in Fig. 3 is that the natural frequency of the tremor mode at high-loop gain is heavily dependent on the limb inertia, m_L, and an equivalent spring, k_L, which is a combination of tendon and interface (flesh) compliances. Thus, the tremor mode frequency is relatively insensitive to the feel system restraints.

The frequency of the feel system mode depends primarily on the control stick inertia (m_F), spring rate (k_F), and interface compliance (k_I). This

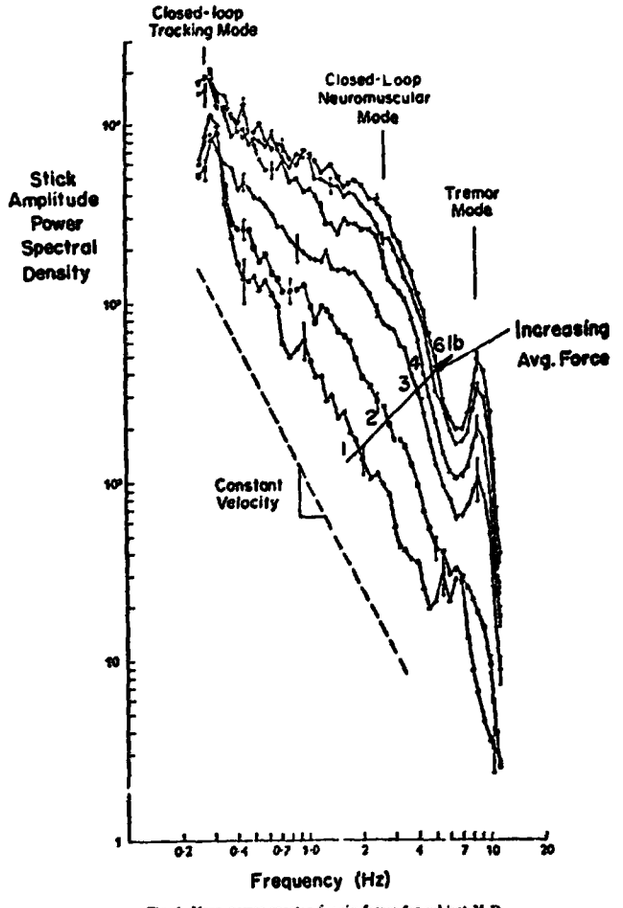

Fig. 1. Mean power spectra for six forces for subject M.D.
The error bars are of total length twice the standard error of the mean. 1 Lb. (0·45 kg) ▲, 2 Lb (0·91 kg) ■, 3 Lb (1·36 kg) +, 4 Lb (1·81 kg) ×, 5 Lb. (2·27 kg) ●, 6 Lb. (2·72 kg) ▼. The dashed line has a slope of 6 db/octave.

Figure 4. Typical Control (Error) Unsteadiness Power Spectra for Various Steady Forces on a Pressure Stick (From Sutton and Sykes, Ref. 9)

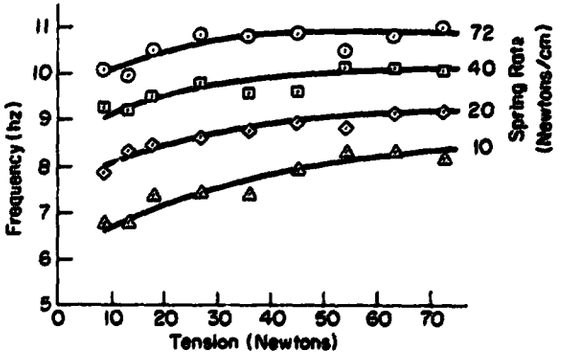

Figure 5. Effects of Set Force and Spring Stiffness on Forearm Flexor Tremor (Adapted from Robson, Ref. 11)

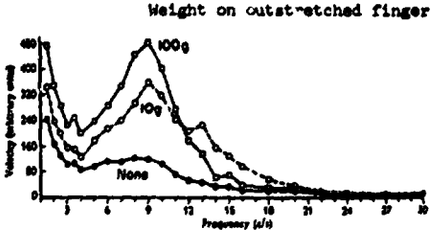

Plotting of tremor measured as velocity versus frequency in cycles per second averaged for the movements of the terminal phalanx of the fingers of 26 normal men. With the unloaded fingers (filled circles) and with 10 g (circle) and 100 g (square) strapped to the terminal phalanx. (Halliday and Redfearn, 1956, Ref. 12).

Figure 6. Effects of Load Weight on Velocity Power Spectral Density

mode may be beyond the frequency region of interest for extremely small inertia and stiff springs; while for large control inertias or weak springs, the feel system modes may be even lower than the tremor modes. Detailed analysis of these situations has yet to be done for this particular model and is beyond the scope of this brief survey.

Data on Unsteadiness Power Spectral Density

We will now re-examine the earlier experimental data on which this model is based from the standpoint of unsteadiness and tremor. The data to be reviewed are easier to interpret having digested the neuromuscular model and dynamics in Figs. 2 and 3.

An example of the error power spectral density for a pressure joystick is shown in Fig. 4 for a range of applied forces from Sutton and Sykes (Refs. 9 and 10). At larger forces the Neuromuscular and Tremor modes are quite distinct. The feel system mode is not within the data band since the feel system spring rate is nearly infinite. The closed-loop tracking mode is near 0.3 Hz (although it is not clearly defined for each curve in Fig. 4). Sutton and Sykes found, for four subjects, that the rms error increased linearly with the commanded (set) force. In addition, they found that as the set force increased the tremor frequency increased slightly but soon reached a limit of about 8.5 Hz.

Robson (Ref. 11) found the same trend in the tremor mode frequency with tension, and he took data for a range of stiff spring rates. In Fig. 5 forearm flexor tremor frequency is plotted as a function of the pressure force at the wrist. This force was exerted against a spring (attached to the wrist) which was oriented parallel to the upper arm. For each spring, increasing the force causes a slight increase in tremor frequency except at the higher tensions where the data level off. However, an increase in spring stiffness produces an incremental increase in tremor frequency which is essentially independent of the set force.

To emphasize tremor frequencies (5-15 Hz), Halliday and Redfearn (Ref. 12) used a lightweight accelerometer mounted on an outstretched (tensed) finger subject to various pressure forces while the hand was on a rest. Figure 6 gives their averaged finger tremor data which show that increasing the load weight on the extended finger leads to more tremor at all frequencies and that the amplitude of the tremor mode near 9 Hz increases more than the surrounding spectra. This implies that a small finger-mounted accelerometer would not attenuate the tremor motions. Figure 7 shows spectra for, and cross-spectra between, the right- and left-hand index finger velocity for three subjects. The peaks are in the range of 7-11 Hz. Also shown is the coherence between right- and left-hand unsteadiness, which is very small, indicating that it is the uncorrelated motor noise in each separate limb rather than a common (central) excitation source which drives the tremor mode. These data indicate that the tremor mode is not just a closed-loop neuromuscular system response to an EEG driving signal, even though the EEG's alpha rhythm has the same frequency range.

Data indicating that the feel system mode can be driven to frequencies lower than the tremor mode can be found in Gydikov (Ref. 13) where the task was to track a ramp input (pursuit display). The subject gripped a handle in his fist and used wrist rotation about the forearm axis to generate his response. Four different load inertias were used, and grip tension was sensed. The dependence of dominant mode frequency on inertia and grip tension is given in Fig. 8. For each inertia there is an increase in frequency as tension increases, whereas for constant tension an increase in inertia causes a decrease in frequency. The low frequencies with the large inertia cases indicate that the feel system mode (Fig. 3) has been driven down and is interacting with muscle activation and closed (outer) loop visual-motor dynamics.

Additional results in Ref. 13 indicate that the dynamic modes of one hand are independent of the other. Specifically, if one hand is controlling a large inertia without pressure, then its dominant frequency can be much less than that of the other hand if it is controlling a small inertia with great pressure. This verifies that the Neuromuscular and the Feel System modes can be strongly dependent on the load and, further, that each limb's neuromuscular system has signal drives independent of the other.

The earlier work of Lippold, et al. (Ref. 14) interpreted the extant data at that time as indicating that tremor was <u>not</u> a response to alpha rhythm. In addition, Lippold, et al., found that fatigue increased and

Fig. 4

Representative tremor spectra from three subjects, showing examples of marked difference (L.C. 40 years, female), slight difference (R.L. 37 years, male) and close similarity between the two hands (J.M. 28 years, male). Each spectrum shows: above, the spectra of tremor of the right (●) and left (○) hands; middle, the cross-spectrum between hands (▽), and below, the coherence between hands (■). (From Marsden, et al., 1969, Ref. 1)

Figure 7. Effects of Right and Left Hand Index Finger on Velocity Power Spectral Density

0005 (1 Um)

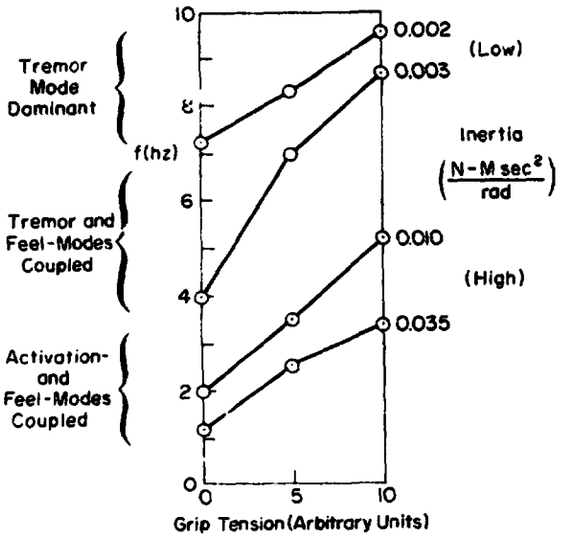

Figure 8. Dominant Frequency Shows Interaction of Feel System and Tremor Modes (Effects of Inertia and Grip Tension on Tremor During Constant Velocity Wrist Rotation, Adapted from Gydikov, Ref. 13)

cooling decreased the tremor frequency; further evidence that the peripheral neuromuscular system determines the tremor mode frequency rather than its being present in a central drive signal. An excellent example of tremor while tracking (involving fine control of position) is provided by some of our unpublished data taken during experiments reported in Ref. 13. This was a multiloop task in which the pilot's feet were controlling rudder pedals and his hand was controlling a stiff spring-restrained side stick. One of the subjects used a high tension technique, i.e., tensed both legs against the pedals and performed the rudder task with differential force changes. Simultaneously, his hand tracking displayed an intermittent tremor of 8 Hz, which was largest at the extreme stick excursions (which requires the largest tensions).

Factors Affecting Tremor

In normal subjects tremor is most often seen when only one muscle is being tensed. That is, for the experiments and data reviewed earlier, in all cases the pilot or subject was producing a force against a restraint (spring or inertia) such that only an agonist muscle was strongly active. Tremor while tracking has always occurred at the extremes of manipulator movement, i.e., where the pilot is pushing with much force against the stick such that only one muscle is being strongly activated, again giving the conditions as above. Tremor while tracking shows an intermittent nature; being easily perceivable only when the pilot is hardover one way or the other. This is readily evident from the time traces. Power spectral analysis of such a run would show some power at the high frequency regions where tremor has been observed, but it would tend to be smeared out due to the intermittent nature of the tremor onset and waning. Thus tremor properties are best measured for cases where the pilot holds a constant force or load weight.

Marsden (Ref. 15), in finger tremor studies, found that the relative size of the tremor peak was correlated with the total rms unsteadiness velocity for both right and left hands. (See Fig. 9.) Here the total rms velocity was evaluated from the total power between 1 and 20 Hz (Fig. 7

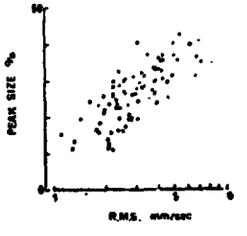

Fig. 9. Relation between the relative size of the peak (ordinate) and total RMS velocity (abscissa) obtained from C.M.'s right (■) and left (▲) hands, and that obtained from J.M.'s right (□) and left (△) hands. Relative peak size increases as tremor increased ($r = +0.33$, $P < 0.01$). (From Marsden, Ref. 15)

indicates that this region contains essentially all the power). The relative peak is defined as the ratio of the power in a 0.5 Hz band about the peak frequency to the total power. In Fig. 9 note that the tremor peak contains an increasing share of the total power as the rms level increases; this is consistent with the data in Figs. 4 a 1 7.

The influence of external factors on tremor per se has been summarized by Marsden (Ref. 15) as follows (underlines ours):

> "The fluctuations in tremor observed in two trained subjects during periods ranging from minutes to months were not great, and the shape of the tremor spectrum was very similar at different times. Many factors are known to contribute to fluctuations in tremor amplitude, including: anxiety (Graham, Ref. 16; Redfearn, Ref. 12), alcoholism (Carrie, Ref. 17), thyrotoxicosis (Lippold, et al., Ref. 18; Marsden, et al., Ref. 19), and fatigue (Eagles, et al., Ref. 20). Some of the fluctuation of tremor amplitude that occurs in the normal subject may be due to variations in catecholamine secretion, for adrenaline infusion has also been found to increase tremor considerably (Marsden, et al., Ref. 21). In addition, the amplitude of tremor is dependent upon the force exerted (Sutton and Sykes, Ref. 9) and, in certain tasks, upon visual feedback (e.g., Sutton and Sykes, Ref. 10); Merton, et al., Ref. 22). All these factors must be taken into account when planning experiments on physiological tremor and when evaluating the results."

In a series of approach and landings with a Boeing 707, Nicholson, et al. (Ref. 23) found significant increases in finger tremor (at 10 Hz) in "stressful" situations ("an unresolved problem persisting or a fresh problem of some magnitude") as evidenced by subjective reports and elevated heart rates (above 150 beats per minute). The finger tremor was measured by a lightweight accelerometer (less than 1 gram) on an outstretched index finger. Fig. 10 shows both pre-takeoff and immediately post-landing tremor spectrum for four of the most stressful cases, in which the dramatic increase in the 10 Hz peak is readily apparent.

Concluding this section on tremor mode properties, the following conclusions are emphasized:

1. The tremor mode is a distinct limb-muscle resonance phenomena, compared to the more highly coupled visual, neuromuscular and feel system modes. As such, it is not strongly correlated with the other visual-motor modes.

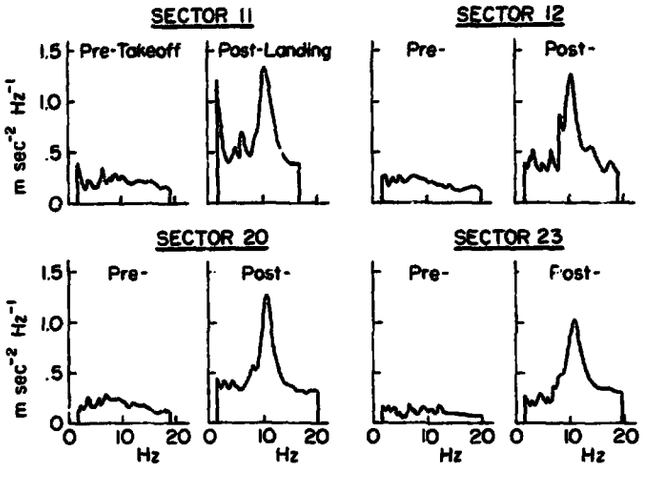

Figure 10. The Frequency Spectra of Finger Tremor for Takeoff (Controls) and for Stressful Landings in Four Letdowns in Which the Mean Heart Rate Exceeded 150 Beats/Min and Was Associated With a Peak Acceleration Around the 10 Hz Frequency Exceeding 1.0 msec^{-2} Hz^{-1} (From Nicholson, et al., 1970, Ref. 23)

2. Its frequency is not very sensitive to limb load and it primarily reflects neuromusoular system feedback lags and tendon compliance.

3. The tremor mode power spectral density is narrowband and its amplitude increases with applied force, as well as various external or internal operator stresses.

4. Tremor is most pronounced when only one muscle of an agonist/antagonist pair is tensed.

5. Tremor mode motions are clearly revealed by measuring the limb acceleration (rather than position) in the frequency range from 8-15 Hz.

Factors Affecting Low Frequency Unsteadines

While the tremor mode is a distinct and isolatable mode, the low frequency control motion spectra have multiple peaks (e.g., closed-loop tracking and neuromuscular modes) which are very sensitive to the manipulator restraint as shown by the Gydikov data of Fig. 8 as well as control stick type. The pressure-stick displacement spectrum in Fig. 4 shows the closed loop tracking mode and the muscle/manipulator mode while these modes are not obvious in the unrestrained finger acceleration spectra (Fig. 7). In tracking tasks the controlled element has a strong effect on the pilot's equalization (Ref. 3) and thereby the frequency and damping of the closed loop tracking mode which results. Furthermore, the forcing function bandwidth, if large, may cause crossover regression thereby lowering the closed loop tracking mode frequency. Thus, the power spectral density of unsteadiness motion is multipeaked, and there is no single pair of frequency-amplitude parameters which can meaningfully describe the signal properties unless bandpass filtering is performed first. If information is desired about all the possible modes of unsteadiness, the best solution is to measure the complete power-spectral-density and carefully analyze it. However, a simpler metric of low frequency unsteadiness is the overall rms position excursions, because for force regulation (Fig. 4), the low frequency modes dominate the displacement PSD. In addition this metric is directly relevant to fine motor task performance, since this is a direct measure of the average closed loop unsteadiness magnitude.

An example of this metric is given by Marsden (Ref. 1). He investigated the correlation between the tremor peak size with low frequency unsteadiness and total rms control velocity (Figs. 11a and 11b). The data (in the range 1-5 Hz) has a small and negative correlation with the tremor mode peak. This indicates that the low frequency modes may have different trends from those of the tremor mode. The positive correlation for the total, Fig. 11b, is consistent with Fig. 9.

Thus, fine-motor task unsteadiness can be assessed separately from the tremor mode by filtering out the high frequency portion of the signal and measuring the rms position excursions in the non-tracking case.

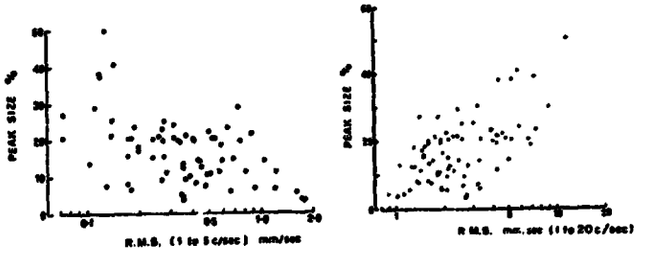

a) Low Frequency Unsteadiness b) Total RMS Unsteadiness

Figure 11. Correlation of Tremor Peak Size with Low Frequency and Wideband RMS Unsteadiness

EXPERIMENT TO VALIDATE RECOMMENDED MEASUREMENTS

Experimental Setup

A simple analog computer simulation was conducted in order to test various unsteadiness measurement concepts suggested in Sections A and B and to validate the tremor and unsteadiness tests recommended therein. A functional block diagram of the simulation is shown in Fig. 12. The subjects were required to rest their elbows on an arm rest and, pulling with the ball of their first finger, null out a command force using a nearly isometric (very stiff) control stick (MSI Model 435). The difference signal c_e represents the control unsteadiness. Force error feedback to the subject was provided by a 5-inch Dumont 304A Oscilloscope. The displayed error was smoothed by a first order filter with a 1.0 second time constant, to eliminate perception of the high frequency unsteadiness and to assure a tight loop closure to remove any residual force drift. The dc display/control gain was 2.5 cm on CRT/Newton on stick.

The low-frequency components of fine motor unsteadiness (visual/motor modes) were measured by the rectified and averaged control error signal, $\overline{|c_e|}$, as shown in Fig. 12.

The tremor mode signals were obtained by processing the control error signal (c_e). The rate and acceleration of c_e were obtained with a pseudo-differentiation circuit. The acceleration signal was additionally smoothed with a second order filter similar to the pseudo-differentiation circuit. The break frequency of both circuits was set at 100 rad/sec (16 Hz) with a damping ratio of 0.7. These settings give a 25% amplitude attenuation at 16 Hz with linear phase shift up to the break frequency. The phase shift characteristics cause minimal phase distortion in the signals up to the break frequency, and the signals appear as though they are merely time delayed by about 0.014 sec for $\dot{c}_e$ and 0.028 sec for the filtered $\ddot{c}_e$ signal. "Average tremor magnitude" was obtained by rectifying and smoothing the $\ddot{c}_e$ signal, as shown.

Ten subjects (including two females) were asked to hold command forces of 5, 10, 15 and 20 newtons (1.12, 2.25, 3.36 and 4.49 lb respectively) with their right forefinger. Data were recorded with a Brush Mk 200 strip chart recorder (100 Hz bandwidth).

Data

Tremor Frequency. A typical recording is shown in Fig. 13. The tremor frequency in the smoothed acceleration signal is clear at all four force levels. However, the 15 and 20 newton cases appear most suitable for measuring tremor frequency with a zero crossing detector.

The velocity trace shows evidence of the closed loop neuromuscular mode as well as the tremor mode. Closer inspection of the 10 newton trace reveals a 2 to 3 Hz frequency combined with the 13 Hz tremor mode, and past describing function measurements have shown the neuromuscular mode to fall into this frequency range (Ref. 2 and Fig. 3 herein).

It is apparent that the smoothed acceleration signal gives a good measure of the tremor mode frequency and amplitude. These data are shown on Fig. 14. The tremor frequency is remarkably constant while the tremor amplitude increases by an order of magnitude. The mean frequency over 40 trials (4 forces × 10 Ss) was 11.6 Hz (73 rad/sec) with a standard deviation of 0.9 Hz. The lowest frequency measured was 9.5 Hz and the highest was 13 Hz. Measurements with the left hand of two subjects gave frequencies

in the same range, but slightly different than their right hand. Thus it is apparent that the tremor mode occurs within a very restricted frequency region in most subjects over a significant range of applied forces. The low end of this frequency range for isometric-stick pulling also matches the finger-free data shown in the preceding section, "Nature of Unsteadiness."

Additional tremor frequency measurements were made to check the tremor mode of other limbs. These were:

- Free hand tremor measured by pointing a miniature flashlight at a photocell,
- Biceps tremor measured by pulling with the arm on a spring restrained bar,
- Leg muscle (quadraceps) tremor measured by pushing with the foot on a spring restrained pedal.

Frequencies measured in the above manner were within the forefinger tremor frequency range reported above. Also, left hand/right hand tremor was comparable for two subjects tested. Thus the tremor mode frequency of a normal human neuromuscular system seems to be a very fundamental physiological property. From the model and dynamics of Figs. 2 and 3, this implies that the ratio of limb inertia to tendon compliance and the neuromuscular loop lags are about the same for all of these cases, or that other limit-cycling phenomena are involved.

Tremor Magnitude. A time trace of the 1-second running average tremor magnitude signal for a typical run is given in the bottom of Fig. 13. Tremor mode magnitude is a direct function of the average applied force, as shown. It was also found to vary significantly from subject to subject. Average tremor magnitudes for each subject and force level were read off the strip chart recordings and are cross plotted in Fig. 14. These data suggest an exponential relationship between tremor intensity and applied force, with the high forces producing much higher tremor magnitude, e.g., $\sigma_T = \sigma_{T_o} + e^{rF}$, where σ_T, σ_{T_o} = total and residual tremor (rms) magnitudes; F = force, r is fitting constants. It seems that as the average muscle force is increased the tremor mode damping ratio drops and/or the motor remnant forcing function increases (a la Weber Law), while its frequency remains roughly constant. (This is consistent with Fig. 3.)

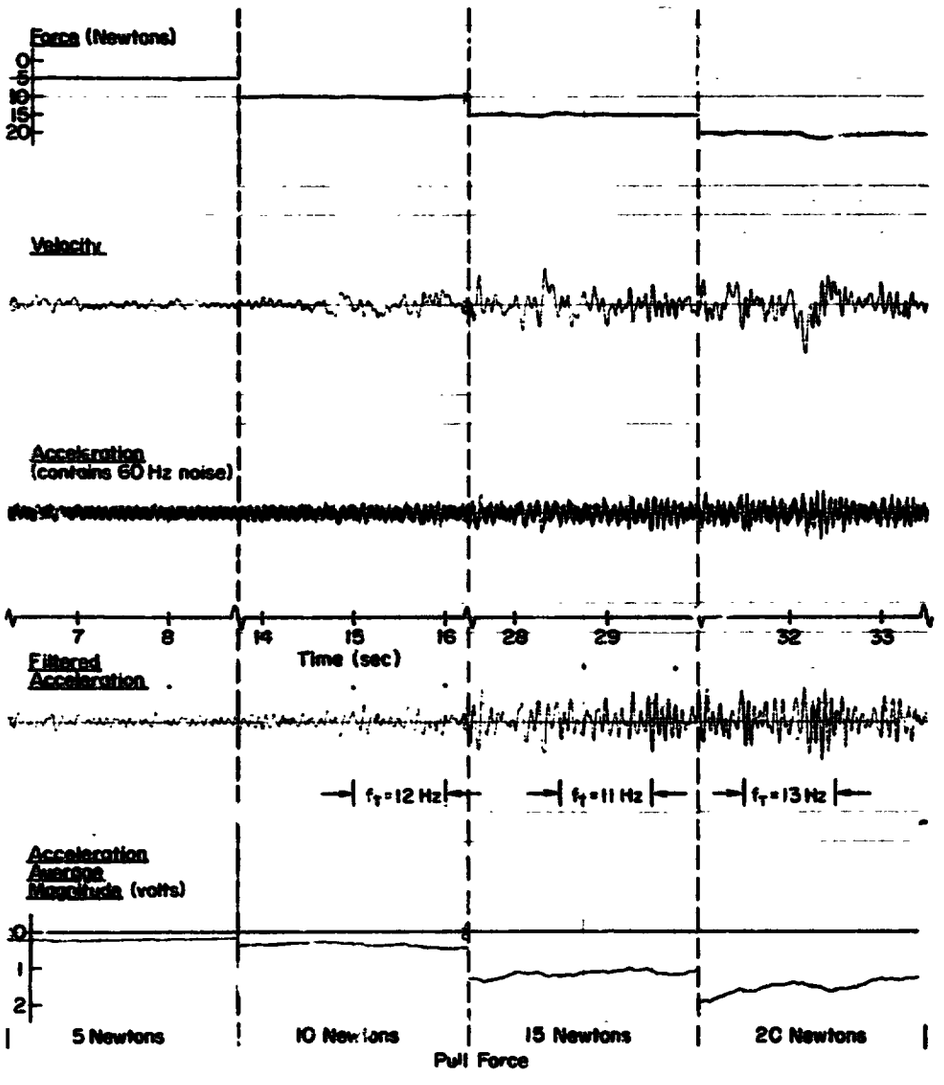

Figure 17. Tremor Test Time Traces for Various Command Forces

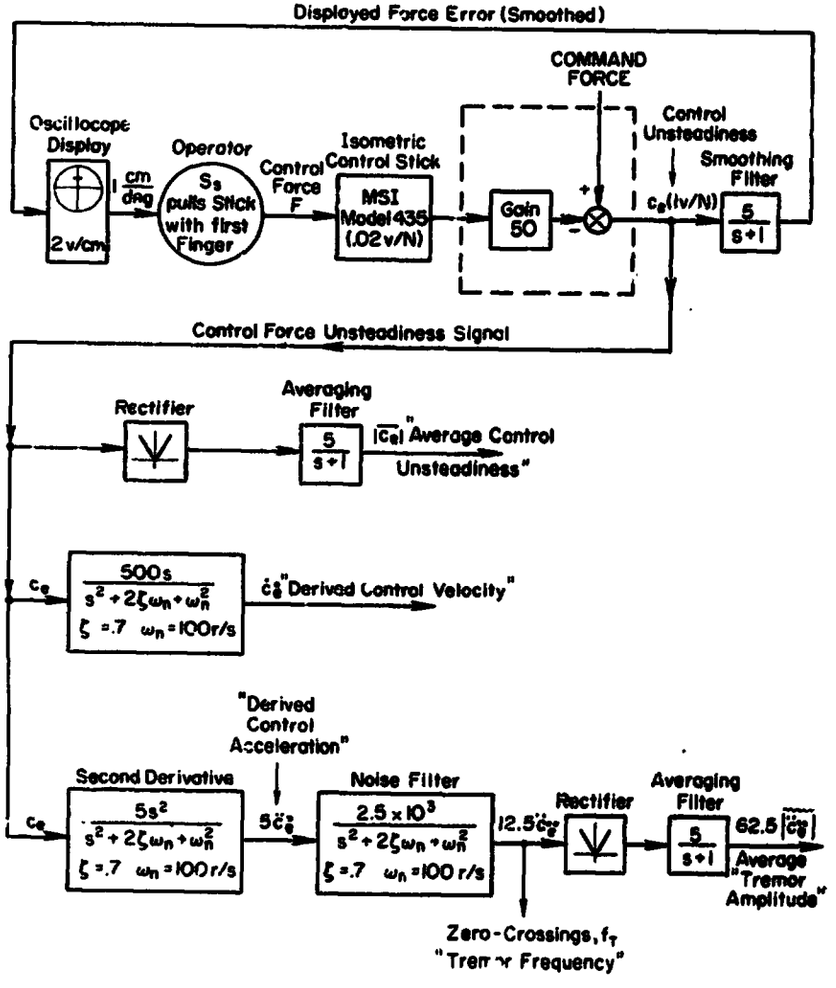

Figure 12. Experimental Setup for Unsteadiness and Tremor Measurements

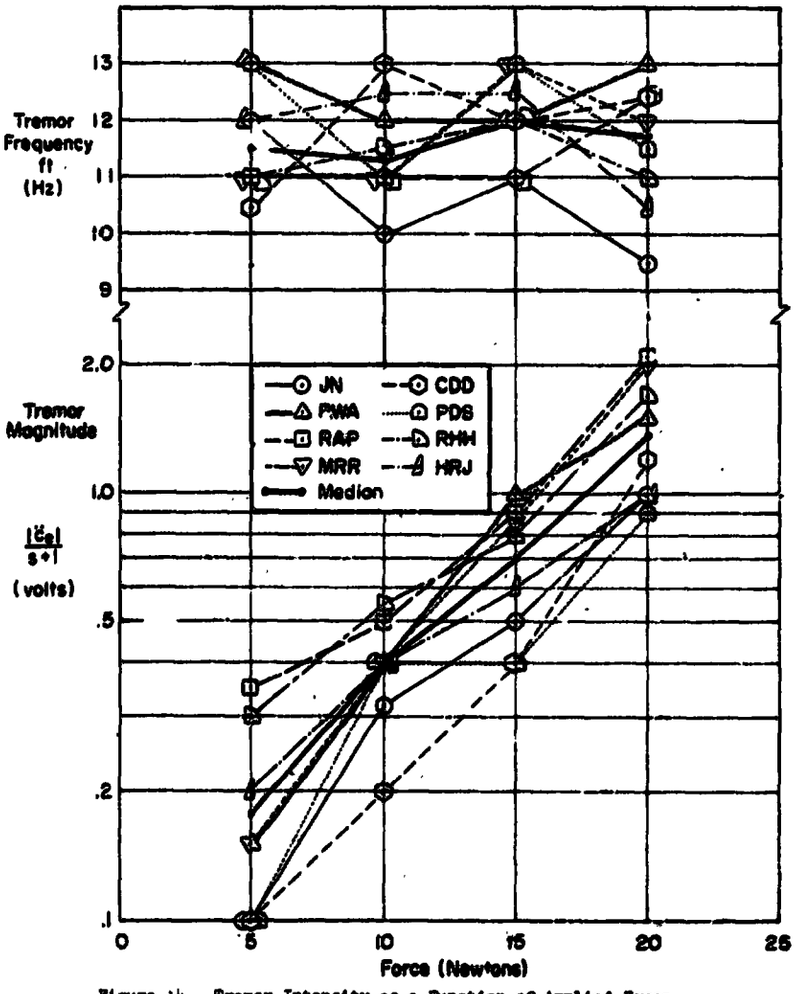

Figure 14. Tremor Intensity as a Function of Applied Force

Unsteadiness Magnitude. A preliminary test was conducted to determine the characteristics of the low-frequency control force unsteadiness signal $|\overline{\ddot{c}_e^*}|$. This measure of unsteadiness magnitude seems to covary somewhat with tremor magnitude and to vary directly with applied force. Low frequency variations also apparent. Additional research will be required to further quantify the characteristics of this measurement.

Standardized Tremor Measures

Based on the success and ease of mechanizing these measures, we recommend the following standard test battery for unsteadiness properties:

- Mechanize the functional circuits shown in Fig. 12 for computing the force error and its derivatives, (omitting derived control velocity). The tremor bandpass filter for computer $\ddot{c}_e^*$ should have $\zeta = 0.7$ for minimal phase distortion and $\omega_n \approx 60$-80 rad/sec to peak near typical tremor frequencies of 9-13 Hz. ("Standard" $\omega_n = 63$ r/s = 10 Hz.)

- Subject presses on the pressure-stick with whatever limb is being investigated, with the limb root grounded (e.g., pull with forefinger; elbow braced). Command forces should be in the range of 5-25 Newtons (1-5 lb) with 15 Newtons (3.4 lb) as a "standard" value for finger pulling.

- Each trial should have a 10 second stabilization period, then 10-second measurement interval. (These periods are a good compromise, balancing measurement precision against muscle fatigue.)

- The test measurements are, in order of interest: "Average Tremor Amplitude" $|\ddot{d}_g^*|$ (which is approximately 1.28 $\sigma_{\ddot{d}_g}$ for a Gaussian signal); "Average Control Unsteadiness," $|\ddot{c}_e|$ (roughly = 1.28 $\sigma_{\ddot{c}_e}$); and the "Average Tremor Frequency" f_t (e.g., from the positive-going axis crossing of the $\ddot{d}_g^*$ signal).

- To make such measures of universal value, the values of c_e and c_g should be given in terms of force or force acceleration (N, N/sec^2), respectively.

CONCLUDING REMARKS

This paper has summarized some recent work in developing a quasilinear model and measurements characterizing the neuromuscular control of a precisely manipulated device such as a: soldering iron, handgun, or various types of manual control sticks, wheels or pedals. The model given here is based on the dominant physiological components and phenomena involved, and it can cover all these cases. In addition, it clearly reveals the various modes of fine-motor unsteadiness, including the Neuromuscular mode at 1-3 Hz and the Tremor mode near 10 Hz. The data review and reexamination, upon which it is based shows good qualitative agreement with many phenomena observed by earlier experimenters, as well as our own work.

Nevertheless, we feel a little uneasy about the "cause" of the very stable-frequency tremor mode. Our brief experiment showed a tenfold increase in tremor amplitude for a fourfold increase in finger pull-force, while the tremor frequency remained within ±1 Hz of 11 Hz, all consistent with the model of Figs. 1-3. Nevertheless, there are other mechanisms, such as threshold-plus-delay-caused limit cycles which might be involved. Furthermore, we have not considered any of the tremor-symptomatic diseases such as Parkinson's Disease, nor have we separated the motor-remnant from the system dynamics. Clearly, more investigation is warranted, using this model as a guide to the appropriate measures and tests.

The proposed "standard" Unsteadiness Test Battery is recommended for clinical investigations of the effects on fine-motor unsteadiness of: various stressors such as work fatigue, lack of sleep, drugs, high-adrenalin situations, and febrile illness; on different limbs; for various ages; and with different manipulated devices. The authors would like to hear about any applications of these tests or modifications to the model.

REFERENCES

1. Marsden, C. D., J. C. Meadows, G. W. Lange, and R. S. Watson, "The Relation Between Physiological Tremor of the Two Hands in Healthy Subjects," Electroenceph. clin. Neurophysiol., 1969, Vol. 27, pp. 169-185.

2. Magdaleno, Raymond E., Duane T. McRuer and George P. Moore, Small Perturbation Dynamics of the Neuromuscular System in Tracking Tasks, NASA CR-1212, Dec. 1968.

3. McRuer, D., D. Graham, E. Krendel, and W. Reisener, Jr., Human Pilot Dynamics in Compensatory Systems — Theory, Models, and Experiments with Controlled Element and Forcing Function Variations, AFFDL-TR-65-15, Jan. 1965.

4. McRuer, D. T. and E. S. Krendel, Dynamic Response of Human Operators, WADC-TR-56-524, Oct. 1957.

5. Levison, William H., David L. Kleinman, and Sheldon Baron, A Model for Human Controller Remnant, Bolt Beranek and Newman, Inc., Rept. 1751, Job No. 11320, 15 Oct. 1968.

6. Clement, W. F., R. W. Allen, and H. R. Jex, Experiments in Controlled Display Scanning and Sampling, NASA CR-1569, July 1970.

7. Magdaleno, R. E., and D. T. McRuer, Experimental Validation and Analytical Elaboration for Models of the Pilot's Neuromuscular Subsystem in Tracking Tasks, NASA CR-1757, April 1971.

8. Magdaleno, R. E., and D. T. McRuer. "A Closed-Loop Neuromuscular System Explanation of Force Disturbance Regulation and Tremor Data," Fourth Annual NASA-University Conference on Manual Control, NASA SP-192, 1969, pp. 527-541.

9. Sutton, G. G., and K. Sykes, "The Variation of Hand Tremor with Force in Healthy Subjects," J. Physiol. (Lond.), 1967b, Vol. 191, pp. 699-711.

10. Sutton, G. G., and K. Sykes, "The Effect of Withdrawal of Visual Presentation of Errors Upon the Frequency Spectrum of Tremor in a Manual Task," J. Physiol. (Lond.), 1967a, Vol. 190, pp. 281-293.

11. Robson, J. G., "The Effect of Loading on the Frequency of Muscle Tremor," J. Physiol., 1959, pp. 29P.

12. Halliday, A. M., and J. W. T. Redfearn, "An Analysis of the Frequencies of Finger Tremor in Healthy Subjects," J. Physiol., Vol. 134, 1956, pp. 600-611.

13. Gydikov, A., "Sampling with Adjustable Frequency in the Hand Movement Control System," IEEE Trans., Vol. MFE-8, No. 2, June 1967, pp. 135-140.

14. Lippold, O. C. J., J. W. T. Redfearn, and J. Vuco, "The Rhythmical Activity of Groups of Motor Units in the Voluntary Contraction of Muscle," J. Physiol. (Lond.), 1957, Vol. 137, pp. 475-487.

15. Marsden, C. D., J. C. Meadows, G. W. Lange, and R. S. Watson, "Variations in Human Physiological Finger Tremor, with Particular Reference to Changes with Age," Electroenceph. clin. Neurophysiol, 1969, Vol. 27, pp. 169-178.

16. Graham, J. D. P., "Static Tremor in Anxiety States," J. Neurol. Neurosurg. Psychiat., 1945, Vol. 8, pp. 57-60.

17. Carrie, J. R. G., "Finger Tremor in Alcoholic Patients," J. Neurol. Neurosurg. Psychiat., 1965, Vol. 28, pp. 529-532.

18. Lippold, O. C. J., J. W. T. Redfearn, and J. Vuco, "The Frequency Analysis of Tremor in Normal and Thyrotoxic Subjects," Clin. Sci., 1959, Vol. 18, pp. 587-595.

19. Marsden, C. D., T. M. D. Gimlette, R. G. McAllister, D. A. L. Owens, and T. N. Miller, "Effect of β-Adrenergic Blockade on Finger Tremor and Achilles Reflex Time in Anxious and Thyrotoxic Patients," Acta endocr. (Kbh.), 1968, Vol. 57, pp. 353-362.

20. Eagles, J. B., A. M. Halliday, and J. W. T. Redfearn, "The Effects of Fatigue on Tremor," In W. F. Floyd and A. T. Welford (eds.), Symposium on Fatigue, Lewis, London, 1953, pp. 41-58.

21. Marsden, C. D., T. H. Foley, D. A. L. Owen, and R. G. McAllister, "Peripheral β-Adrenergic Receptors Concerned with Tremor," Clin. Sci., 1967a, Vol. 33, pp. 53-65.

22. Merton, P. A., H. B. Morton, and C. Rashbass, "Visual Feedback in Hand Tremor, Nature (Lond.), 1967, Vol. 216, pp. 583-584.

23. Nicholson, A. N., L. E. Hill, R. G. Borland and H. M. Ferres, "Activity of the Nervous System During the Let-Down, Approach and Landing: A Study of Short Duration High Work Load," Aero. Med., Vol. 4, pp. 436-466, April 1970.